

# Hybrid anchoring for a color-reflective dual-frequency cholesteric liquid crystal device switched by low voltages

Yu-Cheng Hsiao,<sup>1</sup> Ivan V. Timofeev,<sup>2,3</sup> Victor Ya. Zyryanov,<sup>2</sup> and Wei Lee<sup>1,\*</sup>

<sup>1</sup>*Institute of Imaging and Biomedical Photonics, College of Photonics, National Chiao Tung University, Guiren Dist., Tainan 71150, Taiwan*

<sup>2</sup>*Kirensky Institute of Physics, Siberian Branch of the Russian Academy of Sciences, Krasnoyarsk 660036, Russia*

<sup>3</sup>*Laboratory for Nonlinear Optics and Spectroscopy, Siberian Federal University, Krasnoyarsk 660041, Russia*  
*\*wlee@nctu.edu.tw*

**Abstract:** Cholesteric liquid crystal (CLC) materials used in electro-optical (EO) devices are characterized by high operating voltage and slow response speed, which hinders their further development in display applications. Dual-frequency CLCs (DFCLCs) can solve the problem of slow bistable transition, but the operating voltage is still high, especially in color-reflective DFCLC cells. Here we report a simple approach to lowering the switching voltage as well as to shortening the response time. This technique adopts hybrid surface treatment to modulate the structural arrangement of CLC molecules. Both planar- and vertical-alignment layers are employed and coated on one and the other substrates separately to improve the electro-optical properties of DFCLCs. We show that the threshold voltage for switching can be decreased to as low as 5 V and the shortest response time is measured to be 0.8 ms, which renders CLC EO devices including displays more practical for commercial purpose.

©2015 Optical Society of America

**OCIS codes:** (160.3710) Liquid crystals; (160.1585) Chiral media; (230.2090) Electro-optical devices; (230.3720) Liquid-crystal devices.

---

## References and links

1. X.-Y. Huang, D.-K. Yang, and J. W. Doane, "Transient dielectric study of bistable reflective cholesteric displays and design of rapid drive scheme," *Appl. Phys. Lett.* **67**(9), 1211–1213 (1995).
2. D.-K. Yang, J.-W. Doane, Z. Yaniv, and J. Glasser, "Cholesteric reflective display: drive scheme and contrast," *Appl. Phys. Lett.* **64**(15), 1905–1907 (1994).
3. S.-T. Wu and D.-K. Yang, *Reflective Liquid Crystal Displays* (Wiley, 2001), Ch. 8.
4. P.-T. Lin, X. Liang, H. Ren, and S.-T. Wu, "Tunable diffraction grating using ultraviolet-light-induced spatial phase modulation in dual-frequency liquid crystal," *Appl. Phys. Lett.* **85**(7), 1131–1133 (2004).
5. Y. Yin, S. V. Shiyankovskii, A. B. Golovin, and O. D. Lavrentovich, "Dielectric torque and orientation dynamics of liquid crystals with dielectric dispersion," *Phys. Rev. Lett.* **95**(8), 087801 (2005).
6. Y.-C. Hsiao, C.-Y. Tang, and W. Lee, "Fast-switching bistable cholesteric intensity modulator," *Opt. Express* **19**(10), 9744–9749 (2011).
7. I. I. Smalyukh, B. I. Senyuk, P. Palffy-Muhoray, O. D. Lavrentovich, H. Huang, E. C. Gartland, Jr., V. H. Bodnar, T. Kosa, and B. Taheri, "Electric-field-induced nematic-cholesteric transition and three-dimensional director structures in homeotropic cells," *Phys. Rev. E Stat. Nonlin. Soft Matter Phys.* **72**(6), 061707 (2005).
8. D. Subacius, P. J. Bos, and O. D. Lavrentovich, "Switchable diffractive cholesteric gratings," *Appl. Phys. Lett.* **71**(10), 1350–1352 (1997).
9. I. Gvozдовskyy, O. Yaroshchuk, M. Serbina, and R. Yamaguchi, "Photoinduced helical inversion in cholesteric liquid crystal cells with homeotropic anchoring," *Opt. Express* **20**(4), 3499–3508 (2012).
10. M. R. Lewis and M. C. K. Wiltshire, "Hybrid aligned cholesteric: A novel liquid-crystal alignment," *Appl. Phys. Lett.* **51**(15), 1197–1199 (1987).
11. Y.-C. Hsiao, C.-Y. Wu, C.-H. Chen, V. Ya. Zyryanov, and W. Lee, "Electro-optical device based on photonic structure with a dual-frequency cholesteric liquid crystal," *Opt. Lett.* **36**(14), 2632–2634 (2011).
12. Y.-C. Hsiao, H.-T. Wang, and W. Lee, "Thermodielectric generation of defect modes in a photonic liquid crystal," *Opt. Express* **22**(3), 3593–3599 (2014).
13. Y.-C. Hsiao, C.-T. Hou, V. Ya. Zyryanov, and W. Lee, "Multichannel photonic devices based on tristable polymer-stabilized cholesteric textures," *Opt. Express* **19**(24), 23952–23957 (2011).

14. Y.-C. Hsiao, Y.-H. Zou, I. V. Timofeev, V. Ya. Zyryanov, and W. Lee, "Spectral modulation of a bistable liquid-crystal photonic structure by the polarization effect," *Opt. Mater. Express* **3**(6), 821–828 (2013).
  15. F.-C. Lin and W. Lee, "Color-reflective dual-frequency cholesteric liquid crystal displays and their drive schemes," *Appl. Phys. Express* **4**(11), 112201 (2011).
  16. Y.-C. Hsiao and W. Lee, "Lower operation voltage in dual-frequency cholesteric liquid crystals based on the thermodielectric effect," *Opt. Express* **21**(20), 23927–23933 (2013).
  17. S.-Y. Lu and L.-C. Chien, "A polymer-stabilized single-layer color cholesteric liquid crystal display with anisotropic reflection," *Appl. Phys. Lett.* **91**(13), 131119 (2007).
- 

## 1. Introduction

Cholesteric liquid crystals (CLCs) are a type of optically active liquid crystalline materials having a helical arrangement of molecular directors from layer to layer. They are usually utilized in the form of a thin layer between two parallel substrates in such a way that the helical axis is perpendicular to the substrate surfaces. Conforming to the definition of a circular polarizer, if such a thin CLC layer is irradiated with a beam of unpolarized light, the component of the light which has the same handedness as the CLC chirality will be reflected, whereas the remainder of the light; i.e., the oppositely handed component, is transmitted. Owing to their intrinsic optical bistability and reflection selectivity governed by the Bragg law, the consequent energy-saving feature of CLC displays is especially alluring. Reflective CLC displays are fabricated without the need of a backlight, polarizers, and color filters, enabling the CLC displays to be more processable [1,2]. Unfortunately, a typical electro-optical (EO) CLC device requires high switching voltage and has a long response time. These drawbacks impede expected development of CLC displays [3]. Dual-frequency CLC (DFCLC) materials generally possess positive dielectric anisotropy at low frequencies, while exhibit negative dielectric anisotropy above a certain frequency known as the crossover frequency  $f_c$ . Thus, by switching the frequency of a reasonable voltage from below to above  $f_c$ , the molecular orientation can be substantially changed [4,5]. On the basis of this nature, DFCLCs can switch bidirectionally or reversibly between the planar (P) state and the focal conic (FC) state by means of frequency-modulated voltage pulses, as first demonstrated by Hsiao *et al.* [6]. DFCLCs can also be used for accelerating the switching process. Accordingly, DFCLCs are more promising for display applications except, again, the high operation voltage. Prior studies of CLCs mainly focus on the planar alignment (PA) configuration because of the strong horizontal force rendering the constituent molecules to be assembled in the P state initially. Smalyukh *et al.* distinctively studied the phase diagram of director structures in CLCs in the vertical-alignment (VA) mode; for rubbed VA substrates, only two types of fingerprint textures were observed [7]. Moreover, the VA mode for CLC applications has been proposed in diffraction gratings and beam-steering components [8,9]. Here we use a simple surface-treatment technique to fabricate a hybrid-anchoring (HA) cell [10]. By coating a PA layer on a substrate and a VA layer on the other, we demonstrate that the resulting cell configuration leads to not only faster switching response but also to lower switching voltage. With this HA approach implemented for DFCLC cells, their unique EO properties now make them more attractive for photonic device applications in displays, light modulators, and many others [11–16].

## 2. Experiment

The nematic host material used in this study is MLC2048 (Merck), whose dielectric anisotropy  $\Delta\epsilon$  at room temperature (20 °C) is + 3.2 at 1 kHz and –3.1 at 50 kHz, and the crossover frequency  $f_c$  (where  $\Delta\epsilon = 0$ ) 12 kHz. The chiral dopant (CD) R5011 (Merck) was dispersed in the nematic host at concentrations of 2.49, 2.88, and 3.51 wt% in order to fabricate three types of cells with reflection wavelengths centered at 650 nm (R), 548 nm (G), and 449 nm (B) in the unperturbed HA configuration, respectively. The DFCLCs were introduced into empty HA cells by capillary action in the isotropic phase. Each HA cell was made of a pair of 1.1-mm-thick indium–tin–oxide glass substrates separately covered with rubbed PA (SE-8793 from Nissan Chemical) and VA (AL-8395 from Daily Polymer, Taiwan) layers, yielding a cell gap  $d$  of  $4.0 \pm 0.5 \mu\text{m}$ . Note that the rubbed PA layer allowed

unambiguous identification of the initial quasi-P state. For comparison, we prepared conventional cells with planar anchoring as well. An arbitrary function generator (Tektronix AFG-3022B) was used to supply various frequency-modulated voltages to switch the DFCLC states. A He-Ne laser operating at the wavelength of 632.8 nm was employed in the EO measurement. The transmission spectra of the DFCLCs were acquired with a high-speed fiber-optic spectrometer (Ocean Optics HR2000 + ) in conjunction with a halogen light source (Ocean Optics HL2000). The experimental temperature was fixed at  $25 \pm 1$  °C. Figure 1 shows a schematic of the two optically stable states and the switching between the quasi-P and FC states in a HA DFCLC cell. The low-frequency (1 kHz) voltage  $V_L$  and high-frequency (100 kHz) voltage  $V_H$  permit the reversible switching.

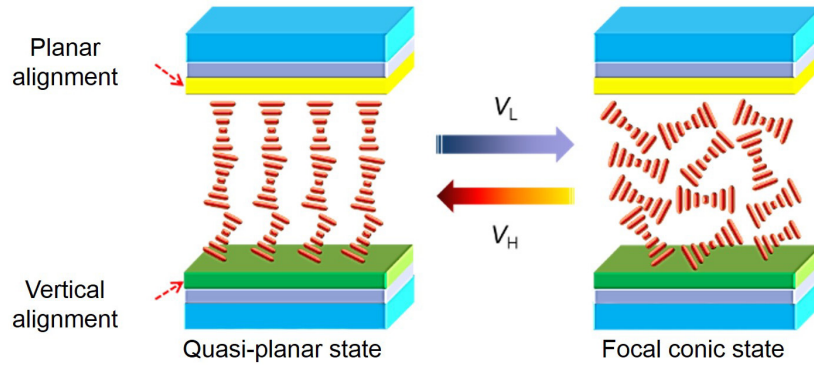


Fig. 1. Schematic of the bidirectional switching in a HA DFCLC cell.  $V_L$ : low-frequency voltage;  $V_H$ : high-frequency voltage.

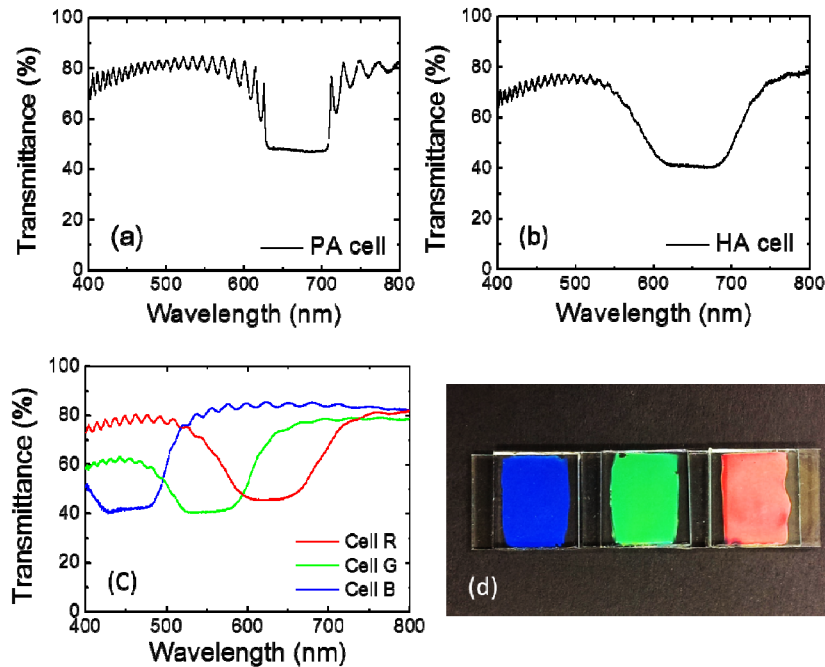


Fig. 2. Transmission spectra of (a) a PA cell and (b) a HA cell containing 2.18-wt% CD in MLC2048 and (c) three HA cells individually composed of CD at 2.49, 2.88, and 3.51 wt%. (d) The appearance of the three HA cells.

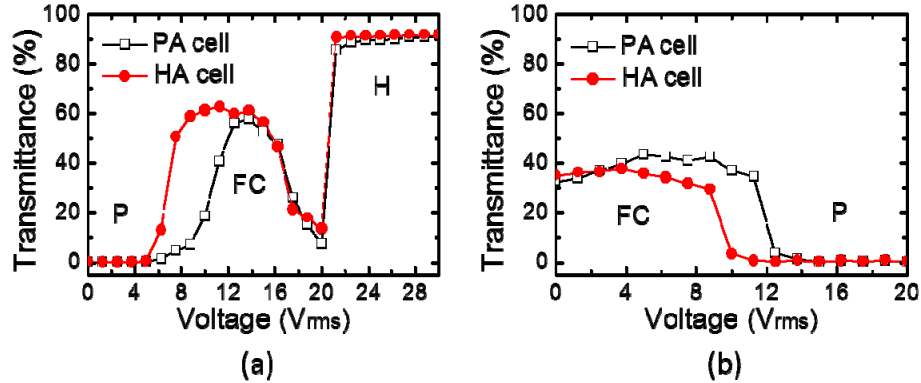


Fig. 3. Voltage-dependent transmittance at operation frequencies of (a) 1 kHz and (b) 100 kHz in cell R of  $4.0 \pm 0.5 \mu\text{m}$  cell gap.

### 3. Results and discussion

Figures 2(a) and 2(b) show the transmission spectra of the DFCLCs (with 2.18-wt% CD and  $4\text{-}\mu\text{m}$  cell gap) in a typical PA cell and a HA counterpart, respectively. The “perfect” Bragg reflection band is revealed in the spectrum of the PA cell as seen in Fig. 2(a). Due to the strong self-assembly and continuum effect, the CLC structure formed in the HA scheme (Fig. 2(b)) also exhibits the Bragg reflection although the reflection band is blunter, with a bandwidth wider than that of the PA cell. Obviously, the CLC molecules are tilted near the VA region, leading to the slight blueshift and broadening of the photonic bandgap [17]. Figure 2(c) shows the transmission spectra of three HA cells with 2.49-, 2.88-, and 3.51-wt% CD dispersed in MLC2048. One can see that the cells reflecting in R, G, and B are demonstrated under the proposed HA configuration (Figs. 2(c) and 2(d)). It is worth mentioning that Fig. 2(d), depicting the appearance of these cells, has not been retouched or manipulated by any photo-editing software. Next we compare the conventional PA and our proposed HA for DFCLC cells. In order to know how the surface treatment affects the operation voltage, EO measurement was taken.

Figure 3(a) illustrates the voltage-dependent transmittance of both the PA and HA cells reflecting in R at the operation frequency of 1 kHz. The transmittance diminishes due to the reflection when the cells are initially in the P or quasi-P state at low voltages. As the low-frequency voltage increases beyond 5 V, the FC state is induced by the broken and randomly oriented helices, allowing photons to transmit via scattering. When the operation voltage elevates further beyond the critical voltage, both DFCLCs transit to the homeotropic (H) state, reaching the maximum in the transmission spectra. Although the critical voltage ( $\sim 21 \text{ V}_{\text{rms}}$ ) is the same for both cells, a 50% reduction in voltage is achieved for P–FC switching in the HA cell— $5 \text{ V}_{\text{rms}}$  solely as compared with  $10 \text{ V}_{\text{rms}}$  for the PA cell, thanks to the VA layer in the HA cell to impose the local distortion and, in turn, to facilitate the transition to the FC state. It is worth mentioning that the  $5\text{-V}_{\text{rms}}$  operation voltage can be easily managed by current thin-film transistors (TFTs). By curiosity, we also found that the switching voltage reasonably increases when the cell gap decreases to  $3.5 \pm 0.5 \mu\text{m}$  in that the strength of PA is usually stronger than that of VA and the anchoring becomes more significant in thinner cells. Likewise, Fig. 3(b) shows that the FC-to-P transition voltages are 9.5 and  $12.4 \text{ V}_{\text{rms}}$  in the HA and PA cells, respectively. Here a 23% reduction is achieved by the rectified surface treatment.

We acquired the reflection spectra of the HA DFCLC cells with a fiber white-light source 20 s after a 100-ms-wide voltage pulse was removed so as to ascertain the bistability. The angle of incidence was  $10^\circ$  from the cell normal and the detector was set at the specular angle. Figure 4(a) delineates the reflections in cells R, G, and B varying with the applied voltage at 1 kHz. Note that the cholesteric texture corresponding to high voltages is quasi-P state owing to

the relaxation from the H state after the removal of the triggering pulses. It is clear that  $V_L = 10 \text{ V}_{\text{rms}}$  induces the “best” scattering states for all of the cells. Figure 4(b) illustrates the reflections in these cells vs. the applied voltage pulse at 100 kHz. It is obvious that  $V_H = 10 \text{ V}_{\text{rms}}$  can generate a strong torque for the HA bulk with negative dielectric anisotropy to be reverted to the quasi-P state. Based on our previous study, the frequency of 100 kHz yields the shortest switching time from the FC to P state [6]. From Fig. 4,  $V_L$  and  $V_H$  can be used for designing the drive scheme in the TFT addressing technology.

Figure 5(a) illustrates the transition times between the FC and P states for a PA cell and a HA counterpart, switched with a  $10\text{-V}_{\text{rms}}$  voltage pulse at 1 kHz for 5 s (as the pulse width). The P–FC response times ( $t_{\text{PF}}$ ) of 1.9 and 0.8 ms were measured in the PA and HA cells reflecting in R, respectively. This is a 58% reduction in response time. Furthermore, the particular property of DFCLC is the response time of the direct FC–P transition ( $t_{\text{FP}}$ ). Figure 5(b) shows that  $t_{\text{FP}}$  are 2.2 and 1 ms for the PA and HA cells, respectively. Here again, a 54% reduction is realized as a result of the modified surface treatment. Table 1 presents the response times,  $t_{\text{PF}}$  and  $t_{\text{FP}}$ , upon a  $10\text{-V}_{\text{rms}}$  pulse for bistable transitions. Since  $V_L$ ,  $V_H$ ,  $t_{\text{PF}}$ , and  $t_{\text{FP}}$  can all be significantly reduced by means of the HA treatment, the issue concerning characteristically high switching voltage in typical DFCLCs can be no more a problem. The added value of the HA for DFCLCs is its even faster response of  $\sim 1$  ms in bistable transitions [6].

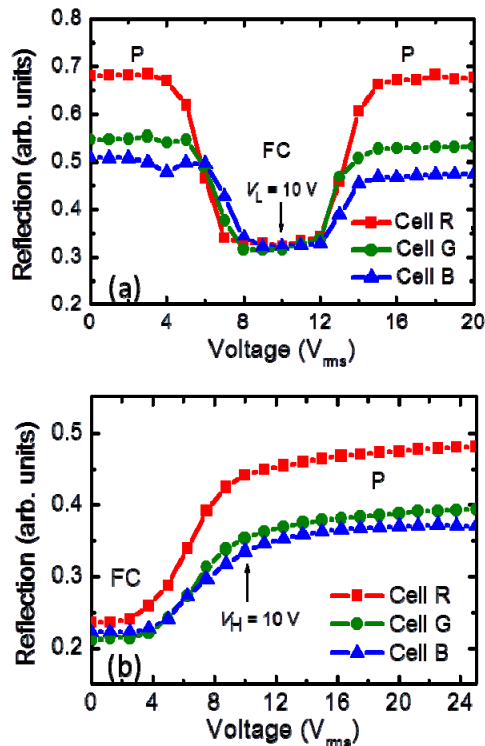


Fig. 4. Reflection intensity of cells R, G, and B vs. the applied voltage pulse at (a) 1 kHz and (b) 100 kHz.

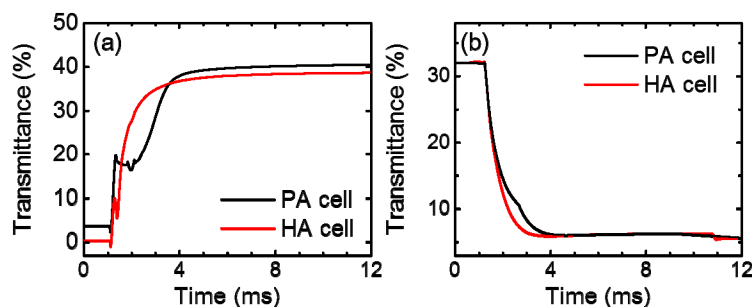


Fig. 5. Optical responses in cells R upon switching at (a) 1 kHz and (b) 100 kHz.

**Table 1. Response Times  $t_{PF}$  and  $t_{FP}$  at 10 V<sub>rms</sub> for HA Cells**

$f$ (kHz)	$t_{PF}, t_{FP}$ (ms)		
	Cell R	Cell G	Cell B
1; 100	0.8; 1.0	2.1; 1.5	2.8; 1.8

#### 4. Conclusions

Interesting EO properties of color-reflective HA DFCLCs have been investigated. The VA layer in a HA cell does not hinder the characteristics of selective reflection and bistability as expected in a typical PA CLC. The optically stable quasi-P state can be rapidly switched to the other stable state—the scattering FC state—by a low-frequency voltage pulse and also rapidly but reversibly back to the quasi-P state by a high-frequency switching voltage. While we previously achieved the fast response in color-reflective CLC display by adopting a DFCLC, enabling the direct and reversible switching between the P state and the FC state [15], here the most prominent improvement by adopting the proposed HA configuration is the much lowered operation voltages for the switching between the bistable states. The fast transition from the quasi-P to FC state is demonstrated with a response time of 0.8 ms. With reasonably low switching voltages and fast response of the order of 1 ms, the HA technique holds great promise for applications in the general CLC device technology. The long-standing problems of the slow response speed and high operation voltages in CLC devices can be simultaneously solved by adopting the HA DFCLC configuration. It thus opens up the possibilities for commercialized DFCLC displays.

#### Acknowledgments

This work was financially sponsored by the Ministry of Science and Technology, Taiwan, under grant No. 103-2923-M-009-003-MY3, by the Russian Foundation for Basic Research (project No. 14-02-31248), and by the Siberian Branch of the Russian Academy of Sciences (SB RAS) through an NSC–SB-RAS joint project between Taiwan and Russia.